SUPPORTING INFORMATION

Engineering lanmodulin's selectivity for actinides over lanthanides by controlling solvent coordination and second-sphere interactions

Joseph A. Mattocks[1], and Joseph A. Cotruvo, Jr.[1*], Gauthier J.-P. Deblonde[2,3*]

[1]Department of Chemistry, The Pennsylvania State University, University Park, Pennsylvania 16802, United States

[2]Physical and Life Sciences Directorate, Lawrence Livermore National Laboratory, Livermore, California 94550, United States

[3]Glenn T. Seaborg Institute, Lawrence Livermore National Laboratory, Livermore, California 94550, United States

*Corresponding Authors: Deblonde1@LLNL.gov (G.J.-P.D.) and juc96@psu.edu (J.A.C.)

Methods section.

Supplementary figures S1 to S13.

Supplementary tables S1 to S5.

Supplementary references.

Methods

Caution! *^{243}Am, ^{239}Np, and $^{248/246}$Cm, as well as their decay products, constitute serious health hazards because of their radioactive and chemical properties. Radiochemical experiments were conducted at LLNL in laboratories designed for the safe handling of short-lived and long-lived radioactive materials and associated waste.*

Materials. ^{243}Am samples were prepared by dilution of a primary standardized stock (Eckert & Ziegler, USA). Curium samples were prepared from a primary source (97% ^{248}Cm + 3% ^{246}Cm) from the LLNL inventory. Neodymium trichloride hexahydrate (>99.9%), europium trichloride hexahydrate (>99.9%), europium acetate monohydrate (99.9%), potassium chloride (>99.95%), sodium chloride (>99.9%), glycine (99.5%), sodium acetate trihydrate (>99%), potassium acetate (>99%), desferrioxamine-B mesylate salt (DFOB, >92.5%), 2-[4-(2-hydroxyethyl)piperazin-1-yl]ethanesulfonic acid (HEPES buffer, >99%), ethylenediaminetetraacetic acid (EDTA, >99%), Ethylene glycol-bis(β-aminoethyl ether)-N,N,N′,N′-tetraacetic (EGTA, >98%), and all other non-radioactive chemicals were purchased from chemical providers (VWR and MilliporeSigma). All solutions were prepared using deionized water (≥ 18.2 MΩ.cm) purified by a reverse osmosis cartridge system (Thermo Scientific).

Protein expression and purification. Wild-type LanM was purified as previously described.[1] The genes encoding LanM variants ($3D_9X$ = D43X/D67X/D92X, where X = A, H, N, or M) were ordered from Twist Biosciences in the pET-29b(+) vector. The variant proteins were expressed and purified as described for the wild-type protein. The selenomethionine-labeled protein was expressed from the $3D_9M$ construct as described by Featherston et al.[2], and the protein was purified as for the other variants, except that 10 mM TCEP was included in purification buffers; the reductant was removed by centrifugal spin column immediately prior to

analysis. Selenomethionine incorporation was assessed by ICP-MS analysis as 2.5 mol Se/mol protein. The yields of the variants (in g/L culture) were: wild-type 60; $3D_9N$ 55; $3D_9A$ 30; $3D_9M$ 30; $3D_9H$ 50; $3D_9$SeMet 13.

Circular dichroism. Samples containing Nd^{3+}, competitive chelator EGTA, and LanM were studied by circular dichroism spectroscopy, using a Jasco J-1500 CD spectrometer, thermostatted at 25 °C, and a 1 mm quartz CD cuvette. A buffered-metal solution of Nd^{3+} and EGTA was prepared as previously described.[1] Briefly, solutions of 20 mM acetate, 100 mM KCl, 10 mM EGTA, 20 μM LanM, ±10 mM $NdCl_3$, at pH 5.0, were mixed in various ratios to produce a range of free Nd^{3+} concentrations. The reference stability constants used for the data refinement were taken from Smith and Martell[3] and selected for the same ionic strength as our study (I = 0.1 M). The pK_a values for EGTA used were: 9.47, 8.85, 2.66, 2.00. In accordance with the literature, the stability constant of the $[NdEGTA]^-$ complex was considered as $\log \beta_{110} = 16.59$ (for I = 0.1 M). The effective K_d ($K_{d,M}$) was calculated to be 12.26 using methods described previously.[1] Samples were incubated for >20 min before measurement to ensure equilibration. CD spectra were acquired between 195 nm and 260 nm, as described.[6] Experimental standard deviations and fitting uncertainties were combined and reported as the total uncertainty.

UV-visible-NIR spectrophotometric titrations. Absorbance spectra of Am(III) samples were measured using a high-performance Cary 6000i UV-vis-NIR spectrophotometer (Agilent Technologies). Samples were contained in sealed quartz cuvettes with a path length of 10 mm (10 mm × 4 mm cells) and the instrument was operated in narrow slits mode (spectral band width = 0.5 nm). Spectra were blank corrected by measuring the absorbance of the corresponding buffer prior to each titration. The initial sample volume was 400-600 μL, depending on the experiment. Instead of preparing separate samples at various LanM/EDTA ratios or separate

samples in various buffers, sequential additions of LanM, EDTA, or acid were performed in order to minimize radioactive material consumption and radiochemical exposure. The duration between each addition was at least 15 min and each titration lasted at least 4 h. At least two independent replicates were performed. All spectra were corrected for dilution. The data treatment was performed with the computer program HypSpec[7] and has been detailed elsewhere.[8,9] The reference stability constants used for the data refinement were taken from the NIST Critical database[4] and selected for the same ionic strength as our study (0.1 M, K^+). The pK_a values for EDTA are: 9.52, 6.13, 2.69, 2.00. In accordance to the literature[4,5], the stability constant of the $[AmEDTA]^-$ complex was considered as $\log \beta_{110} = 16.9$ (for $I = 0.1$). The reported uncertainties in K_d values corresponds to the standard deviation observed between the replicates (experiments + fitting procedure). The usual formalism used in biology for protein binding corresponds to dissociation constants "K_d," whereas global formation constants "β_{MLH}" are generally used to characterize small-molecule complexes. The conversion between the two scales has been previously reported.[8–10]

General methods for fluorescence measurements. a) Curium. For experiments involving actinides, steady-state and time-resolved fluorescence spectra were measured with a FLS1000 spectrometer (Edinburgh Instruments) equipped with a double monochromator on the excitation arm and emission arm. A 450 W Xenon lamp was used as light source for the steady-state measurements and a 60 W microsecond flashlamp was using for lifetime measurements (MCS mode). Each lifetime decay curve contains 2,000 data points, with the maximum count per channel set to at least 1,000. The timespan of the acquisition was set so that the signal was measured until its return to background level. All fluorescence data were measured in sealed

quartz cuvettes and the emission was collected at 90° relative to the excitation. Lifetimes were fitted using the Fluoracle computer program (Edinburgh Instruments).

b) Europium. For experiments involving lanthanides only, steady-state and time-resolved fluorescence data were collected with a Fluorolog-QM fluorometer in configuration 75-21-C (Horiba Scientific) equipped with a double monochromator on the excitation arm and single monochromator on the emission arm. A 75 W Xenon lamp was used as the light source for steady-state measurements and a pulsed Xenon lamp was used for lifetime measurements. All fluorescence data were collected in quartz cuvettes and the emission was collected at 90° relative to the excitation. Lifetimes were fitted using FelixFL software (Horiba Scientific).

Fluorescence spectroscopy metal titrations (Eu^{3+}). The metal-binding stoichiometry of the Eu-LanM complexes (Wild-Type, $3D_9N$, $3D_9A$, $3D_9M$, $3D_9H$, $3D_9SeMet$) was investigated fluorometrically by taking advantage of the protein complex's luminescence. For each variant, 20 μM solution of protein (600 μL) was prepared in 20 mM acetate, 100 mM KCl, pH 5.0 buffer. The protein solution was titrated with 3 μL additions of a 1.5 mM Eu^{3+} stock solution and peak fluorescence was followed at 615 nm (λ_{ex} = 394 nm, λ_{em} = 560-650 nm, integration time = 0.5 sec, step size = 1 nm). The equivalence point of each titration was indicated by the signal at 615 nm remaining constant after multiple additions of Eu^{3+}.

Fluorescence spectroscopy pH titrations (Cm^{3+}). A primary sample containing ~40 μM of Cm^{3+} and 20 μM of protein was prepared for each LanM variant, ensuring complete complexation of Cm^{3+}. For each variant, a small aliquot of the primary sample was then diluted in 15 individual pH buffers to constitute series of samples with pH ranging from 1.0 to 8.3. The final concentrations in the samples were 1 μM Cm and of 0.5 μM LanM variant. Buffers were as follows: 100 mM HCl (pH 1), 25 mM glycine + 75 mM KCl (pH 1.9 to 3.3), 25 mM acetate +

75 mM KCl (pH 3.9 to 5.6), 25 mM HEPES + 75 mM KCl (pH 6.6 to 7.6), 25 mM Tris + 75 mM KCl (pH 8.3). Samples were equilibrated for at least 1 h and then their excitation spectra (λ_{em} = 602.5 nm), emission spectra (λ_{ex} = 399.0 nm), and fluorescence lifetimes were measured. We recently reported[10] the corresponding results for WT LanM.

Fluorescence spectroscopy pH titrations (Eu^{3+}). The pH stability of Eu_2LanM complexes were evaluated fluorometrically by following the Eu^{3+} fluorescence emission at 615 nm (λ_{ex} = 394 nm, λ_{em} = 560-650 nm, integration time = 0.5 sec, step size = 1 nm). Buffers containing 100 mM KCl were prepared at the following pH values using various buffering agents: 1.00 (100 mM HCl); 2.00, 2.30, 2.50, 2.75, 3.33, 3.66 (20 mM glycine); 4.00, 4.33, 4.66, 5.0 (20 mM acetate); 6.0 (20 mM MES); 7.0 (20 mM MOPS); and 8.0, 8.33 (20 mM HEPES). A stock solution containing LanM and 2 eq. of Eu^{3+} (to ensure complete complexation of the metal) was diluted to 0.5 μM LanM in each buffered sample. Each mixture's fluorescence spectrum was measured (λ_{ex} = 394 nm, λ_{em} = 560-650 nm); peak intensity at 615 nm was plotted vs. pH and fitted to the Hill equation. Standard deviation of experimental data was combined with fitting uncertainty and reported as total uncertainty.

Fluorescence spectroscopy titrations with competing chelators (Cm^{3+}). Samples containing Cm^{3+}, LanM, and the buffer were prepared and equilibrated for 30 min. Their excitation spectra (λ_{em} = 602.5 nm), emission spectra (λ_{ex} = 399.0 nm), and luminescence lifetimes were measured. Detailed experimental conditions, with Cm^{3+}, LanM, chelator concentrations, and buffer are given in the figure legends. Fresh stock solutions of the competing chelator (*i.e.*, EDTA or DFOB) were prepared in the corresponding buffer. Incremental additions of chelator were performed, and each addition was followed by fluorescence measurements. The time between each addition of the competing chelator was 15 min; measurements at longer intervals showed

that the sample had reached equilibrium within this time. Each titration lasted about 4 h. The resulting spectra were corrected for the dilution induced by the sequential additions of chelator (the total added volume was typically <15% of the initial volume).

Lifetime measurements in D_2O-H_2O mixtures (Cm^{3+}). The influence of the deuterium/hydrogen ratio in aqueous solvent on the fluorescence lifetime of Cm^{3+} in Cm-LanM complexes was determined as follows, for each of the five LanM variants ($3D_9N$, $3D_9A$, $3D_9M$, $3D_9H$, $3D_9SeMet$). A sample containing 1 μM Cm^{3+} and 0.5 μM LanM variant (ensuring complete complexation of the metal) was prepared in a 100% H_2O matrix (Buffer: 10 mM HEPES, 90 mM NaCl, pH 7.0). Each Cm-LanM variant sample was sequentially diluted with 99.9% D_2O (Sigma Aldrich), constituting, for each variant, a series of nine D_2O-H_2O binary mixtures, from 0% D_2O to 80% D_2O. For each of nine D_2O-H_2O mixture and for each LanM variant, the excitation and emission spectra were measured to verify that the Cm-LanM complex was formed, and its lifetime was measured (λ_{ex} = 399.0 nm, λ_{em} = 602.5 nm). Each lifetime measurement contained 2,000 data points and had a maximum count per channel set to at least 1,000. Lifetimes were fitted using the Fluoracle computer program (Edinburgh Instruments). We recently reported[10] the corresponding results for WT LanM.

Lifetime measurements in D_2O-H_2O mixtures (Eu^{3+}). These measurements were carried out using established methods.[11,12] Solutions of 40 μM Eu^{3+} and 20 μM LanM (Eu_2LanM) were prepared in 100% H_2O matrix (Buffer: 20 mM MOPS, 100 mM KCl, pH 7.0). Half of this initial 100% H_2O Eu_3LanM mixture (2.5 mL) was retained for future use while the remainder was dehydrated by lyophilization. The residual solid was rehydrated in and equivalent amount 99.9% D_2O, lyophilized again, and resuspended a second time in an equivalent amount of 99.9% D_2O. These two Eu_2LanM solutions (100% H_2O or ~99.9% D_2O) were mixed in varying ratios to

produce D_2O contents of 0%, 25%, 50%, 75%, and 99.9%. For each mixture, the lifetime was measured (λ_{ex} = 394 nm, λ_{em} = 615 nm) with 2000 shots over a time span of 2500 μs. Final uncertainty values were propagated from experimental uncertainty.

Curium/lanthanide competitions. Samples containing 1 μM Cm and 0.5 μM LanM (wild-type or $3D_9N$ variant) were prepared at pH 2.9 (25 mM glycine + 75 mM KCl buffer). Eu^{3+} or Nd^{3+} (solution prepared in the same buffer) were added incrementally, creating series of 9 samples, with up to 20 equivalents of Eu^{3+} or Nd^{3+} relative to Cm^{3+}. A reference sample containing only Cm^{3+} (without LanM) was also measured. Samples were equilibrated at least 15 min between additions and the entire titrations lasted ~3 h. Between additions of Eu^{3+} or Nd^{3+}, the emission spectrum of the sample was measured (Emission window = 560-640 nm, λ_{ex} = 399 nm). The amounts of free Cm^{3+} and LanM-bound Cm^{3+} were calculated based on the measured intensity of the Eu/Cm/LanM samples relative to the sample without Eu^{3+}, as well as the reference Cm^{3+} sample. Similar calculations were performed for experiments with Nd^{3+}. The amount of Eu bound to LanM was calculated by mass balance. The separation factor, SF, were calculated as follows:

$$SF(Cm/Eu) = \frac{[Cm\ bound\ to\ LanM]}{[Free\ Cm]} \times \frac{[Free\ Eu]}{[Eu\ bound\ to\ LanM]}$$

Supplementary Figures and Tables

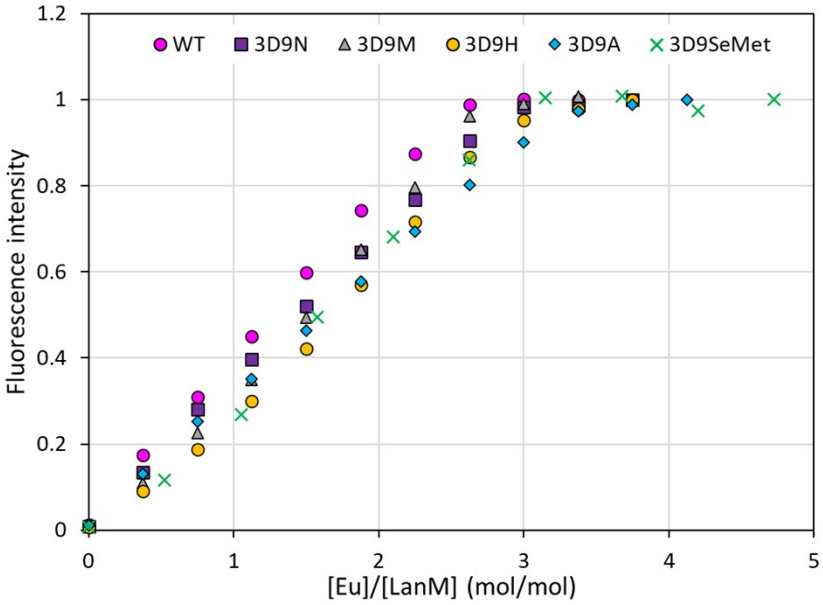

Figure S1. Fluorescence intensity (615 nm) for Eu^{3+} samples containing LanM variants (WT, $3D_9N$, $3D_9A$, $3D_9M$, $3D_9H$, or $3D_9$Se-Met) samples as a function of the ratio Eu/LanM. pH = 5.0.

Table S1. Apparent K_d values ($K_{d,app}$) and Hill coefficients (n) for Nd^{3+} complexes of wild-type LanM and variants, determined by circular dichroism. These results correspond to **Figure 2** for Nd-EGTA-LanM titrations. pH = 5.0. Uncertainties (in parentheses, for 3 experiments) were calculated by combination of fitting uncertainties with experimental standard deviation.

LanM variant	$K_{d,app}$ (pM)	n [b]	Initial [Θ] (deg cm^2 dmol^{-1} × 10^{-3})	Final [Θ] (deg cm^2 dmol^{-1} × 10^{-3})	Fold Change
Wild-type[a]	21.3(0.6)	3.1(0.8)	-518(36)	-1140(80)	2.2(0.2)
	4070(1050)	0.7(0.6)	-1140(80)	-1410(100)	1.2(0.1)
$3D_9N$	53.1(1.9)	1.9(0.2)	-804(25)	-1530(10)	1.9(0.1)
$3D_9A$	397(6)	2.2(0.2)	-508(14)	-1260(10)	2.5(0.1)
$3D_9M$	1460(70)	2.6(0.8)	-531(56)	-1360(50)	2.6(0.3)
$3D_9$SeMet	1160(130)	2.2(0.5)	-606(30)	-1480(40)	2.4(0.1)
$3D_9H$	2150(380)	1.1(0.2)	-505(39)	-1450(50)	2.9(0.2)

[a] Two events. The tighter, cooperative event reflects EF2/EF3, and the weaker event reflects metal binding to EF1.[12]

[b] Note that, while all variants bind 3 equiv. Ln^{3+} (Figure S1), the CD data provides *apparent* K_d values and Hill coefficients for the metal-induced conformational change. Because EF1 responds independently of EF2/3, Hill coefficients ~2 (WT, Ala, Met, and SeMet variants) most likely only reflect the EF2/3 conformational change, while EF1's conformational change may be suppressed even though metal is bound, as is EF hand is poorly responsive even in the WT. The Asn variant is partially pre-ordered in the apoprotein. The $3D_9H$ variant has a Hill coefficient ~1, indicating that the conformational changes are not cooperative.

Table S2. Conversion of K_d values to log β_{MLH} values. The usual formalism used in biology for protein binding corresponds to dissociation constants "K_d," whereas global formation constants "β_{MLH}" are generally used to characterize small-molecule complexes. For clarity, we here provide a conversion of the K_d to log β_{MLH} for the LanM complexes mentioned in the present study. The conversion formula between the two scales has been previously reported.[8–10]. Formula: $\log \beta_{M3LanM} = -\log [Kd_{EF1} \times Kd_{EF2} \times Kd_{EF3}] = -3 \times \log [Kd_{average}]$.

LanM variant	$K_{d,average}$ **for Am_3LanM (in pM)**	**log β_{31} (Am_3LanM)**	$K_{d,app}$ **for Nd_3LanM (in pM)**	**log β_{31} (Nd_3LanM)**
Wild-type	1.4	35.6	21.3 (EF2/3) 4070 (EF1)	29.7
$3D_9$N	3.4	34.4	53.1	30.8
$3D_9$A	9.7	33.1	397	28.2
$3D_9$M	17.1	32.3	1460	26.5
$3D_9$SeMet	16.4	32.4	1160	26.8
$3D_9$H	13.4	32.6	2150	26.0

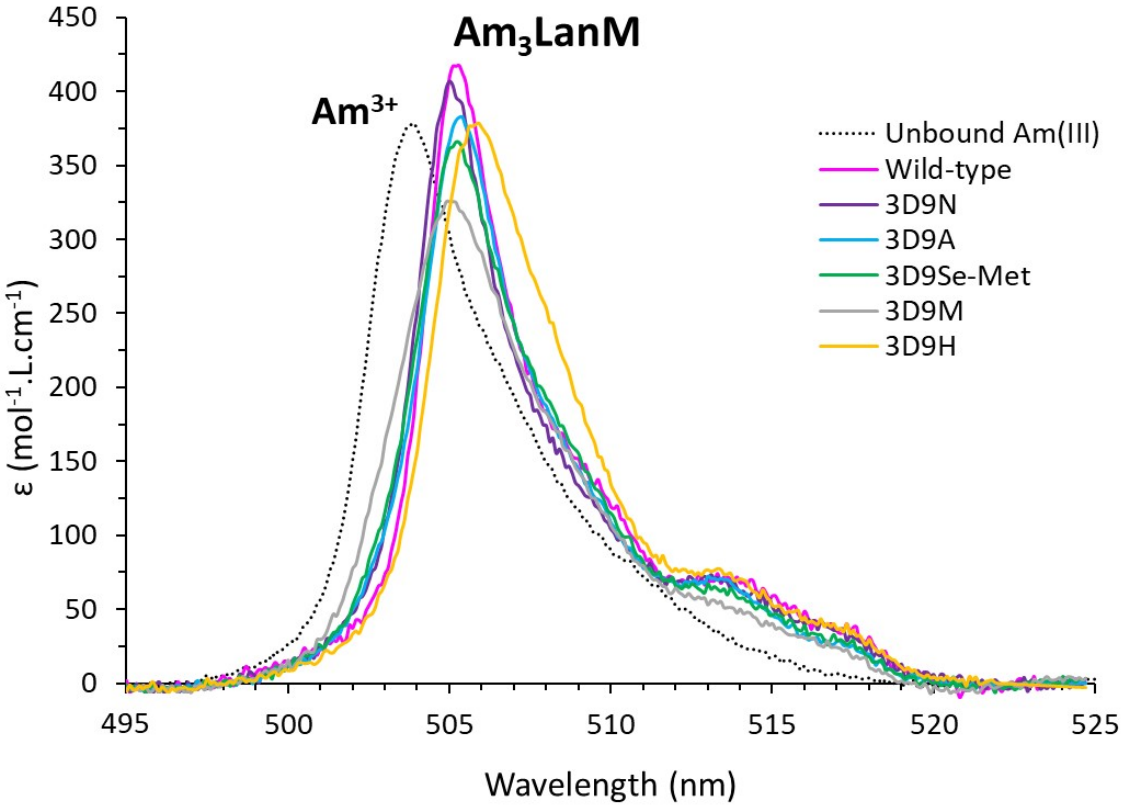

Figure S2. Absorbance properties of the Am_3LanM complexes. Solid curves: UV-visible absorbance spectra of Am(III) when bound to wild-type LanM and its variants $3D_9N$, $3D_9A$, $3D_9SeMet$, $3D_9M$, and $3D_9H$. Dotted curve: Spectrum of unbound Am(III), for comparison. pH = 5.0. Buffer: 25 mM acetate, 75 mM KCl. T = 22 °C.

Table S3. UV-visible absorbance properties of the Am_3LanM complexes and comparison with unbound Am(III) under the same conditions. pH = 5.0. Buffer: 25 mM acetate, 75 mM KCl. T = 22°C. See **Figure S1** for spectra.

LanM variant	**Position of the main f-f transition for Am(III) (λ_{max}, nm)**	**Peak shoulder (range, nm)**	**Width at half height (nm)**	**Extinction coefficient at λ_{max} ($mol^{-1}•L•cm^{-1}$)**
Wild-type	505.2	512-519	3.5	417
$3D_9N$	505.0	512-519	3.6	407
$3D_9A$	505.4	512-519	4.0	382
$3D_9M$	505.0	512-519	5.5	325
$3D_9SeMet$	505.2	512-519	4.6	366
$3D_9H$	505.9	512-519	4.4	378
Unbound Am^{3+} (No LanM)	503.9	none	4.8	379

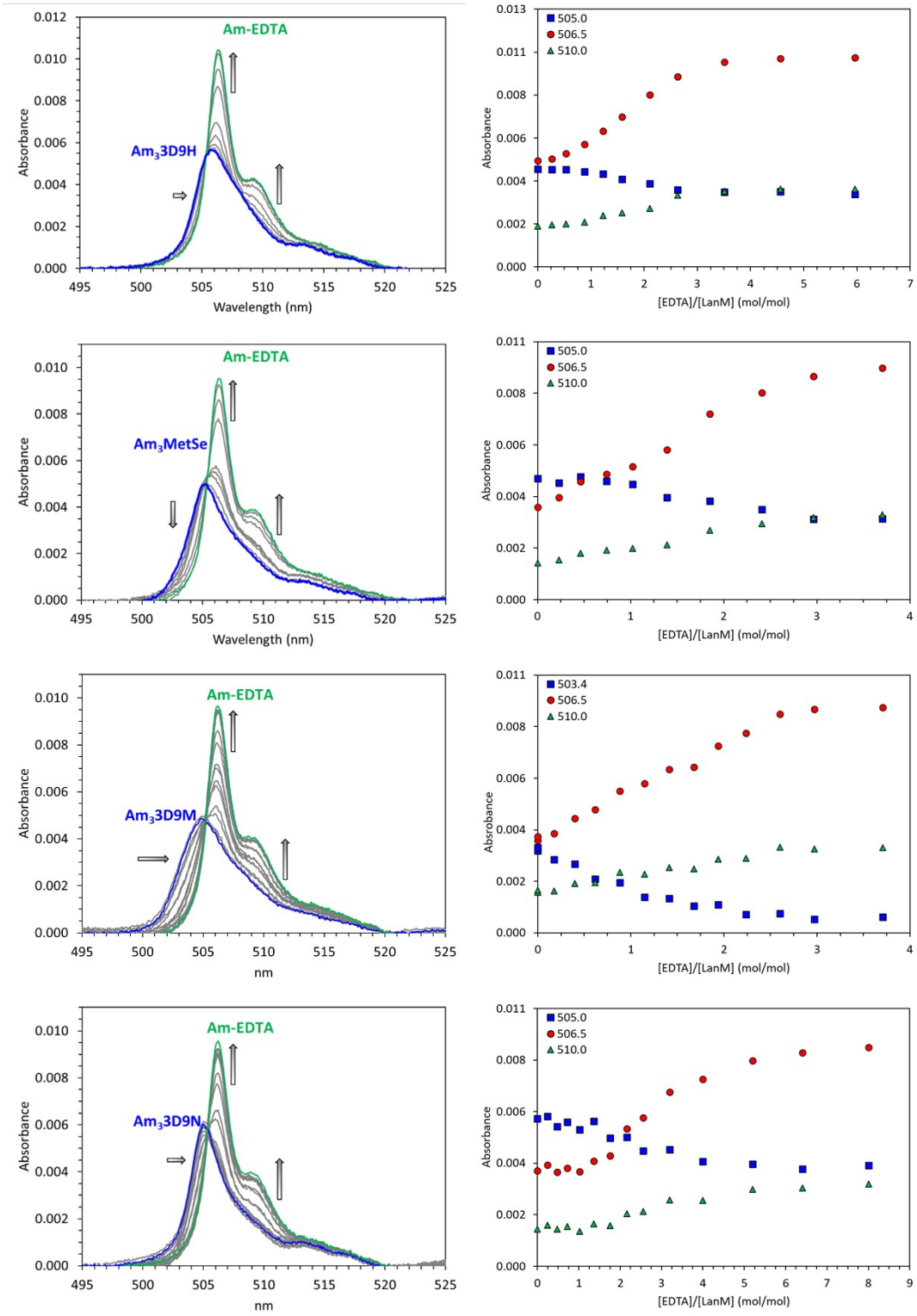

Figure S3. Example of UV-vis spectrophotometric competition titrations of Am(III) complexes of LanM variants (from top to bottom: $3D_9H$, $3D_9SeMet$, $3D_9M$, and $3D_9N$) using EDTA. pH = 5.0. Buffer: 25 mM acetate, 75 mM KCl. See main text and **Figure 2** for equivalent date with the $3D_9A$ variant. Our team previously reported[10] the affinity of wild-type LanM for Am(III) using the same method.

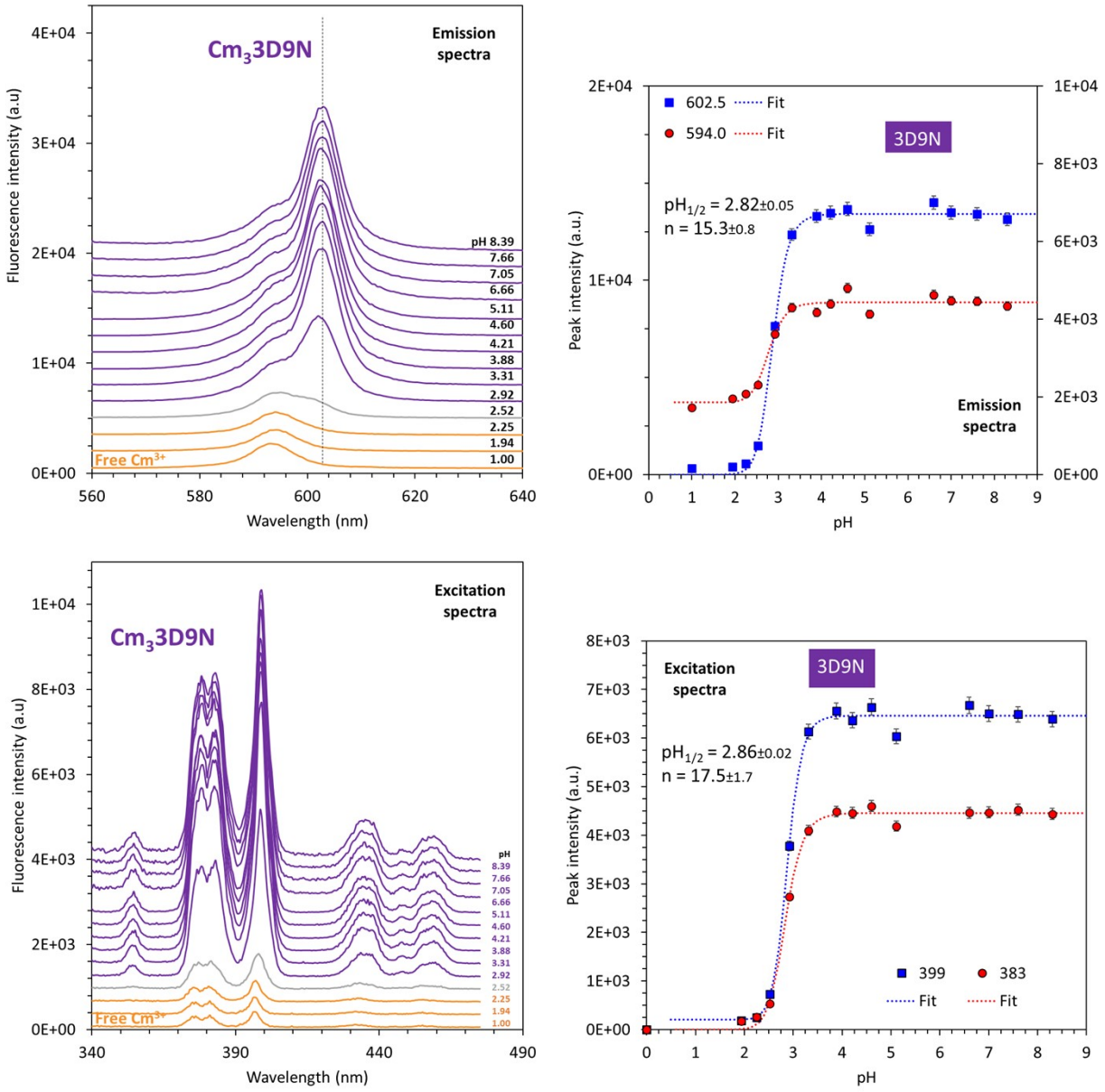

Figure S4. Fluorescence spectra of Cm(III) in the presence of the LanM variant 3D$_9$N and as a function of pH. Top panels = emission. Bottom panels = excitation. For clarity, spectra are stacked, with increasing pH from bottom to top. Right panels represent the measured fluorescence intensity as a function of pH and the corresponding fit results using the Hill equation. The spectral variations as a function of pH were fitted using the two main bands for the emission spectra (594 and 602.5 nm) and excitation spectra (383 and 399 nm). The values given are the average of the two displayed fits. The large *n* values confirm that the protein releases multiple metals, each from sites with multiple titrable ligands, under these conditions.

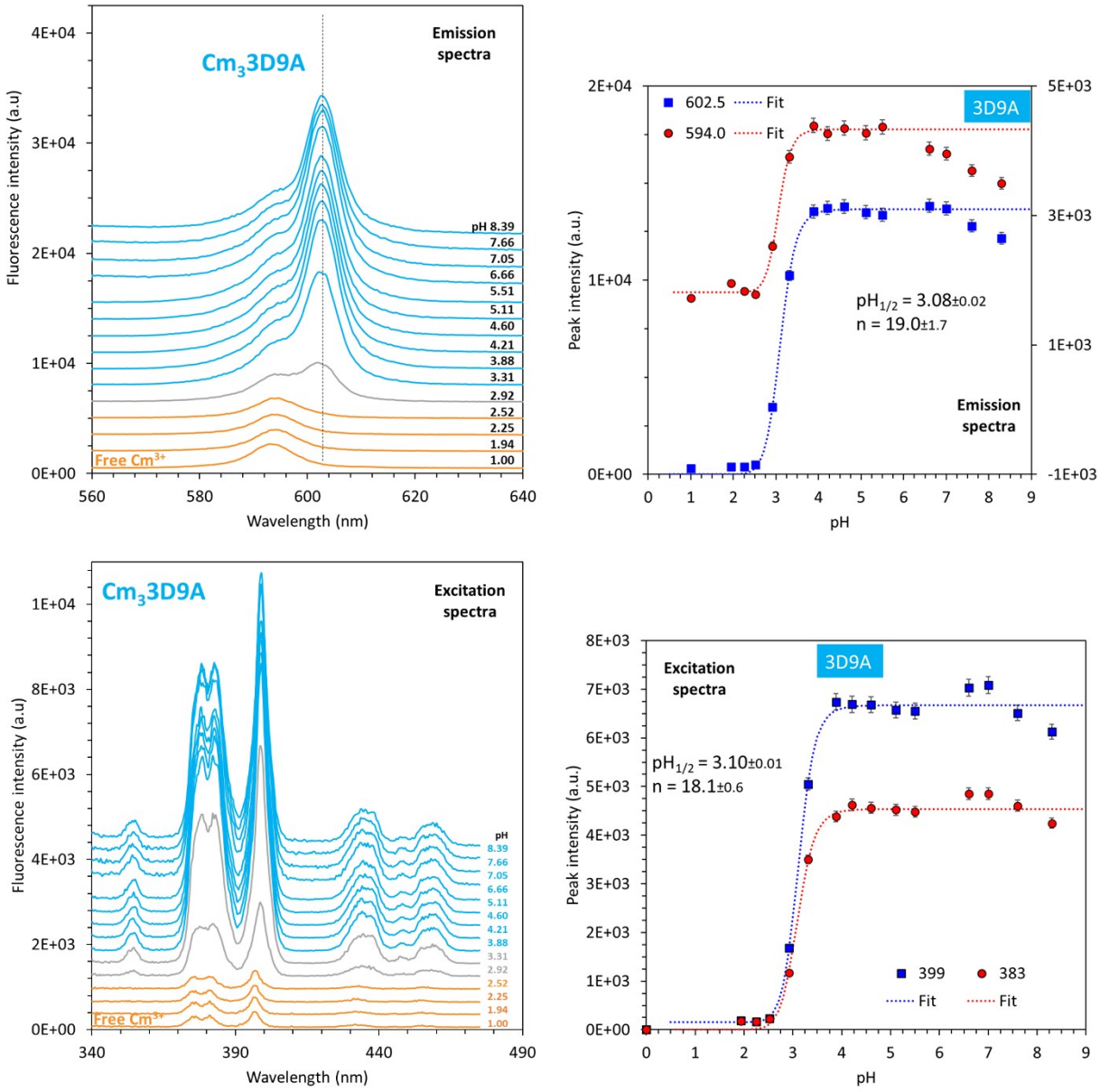

Figure S5. Fluorescence spectra of Cm(III) in the presence of the LanM variant 3D$_9$A and as a function of pH. Top panels = emission. Bottom panels = excitation. For clarity, spectra are stacked, with increasing pH from bottom to top. Right panels represent the measured fluorescence intensity as a function of pH and the corresponding fit results using the Hill equation. The spectral variations as a function of pH were fitted using the two main bands for the emission spectra (594 and 602.5 nm) and excitation spectra (383 and 399 nm). The values given are the average of the two displayed fits. The large *n* values confirm that the protein releases multiple metals, each from sites with multiple titrable ligands, under these conditions.

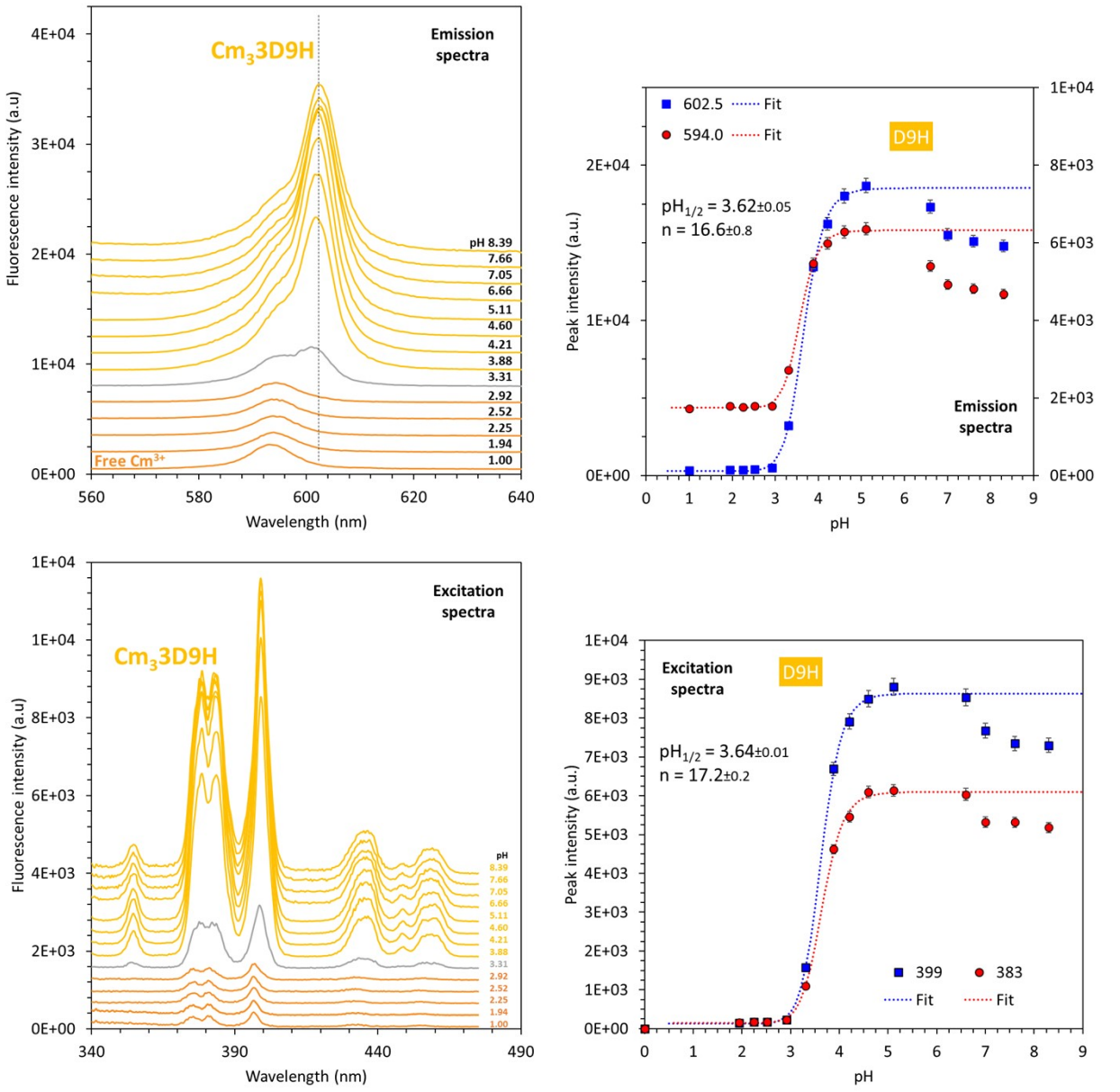

Figure S6. Fluorescence spectra of Cm(III) in the presence of the LanM variant $3D_9H$ and as a function of pH. Top panels = emission. Bottom panels = excitation. For clarity, spectra are stacked, with increasing pH from bottom to top. Right panels represent the measured fluorescence intensity as a function of pH and the corresponding fit results using the Hill equation. The spectral variations as a function of pH were fitted using the two main bands for the emission spectra (594 and 602.5 nm) and excitation spectra (383 and 399 nm). The values given are the average of the two displayed fits. The large *n* values confirm that the protein releases multiple metals, each from sites with multiple titrable ligands, under these conditions.

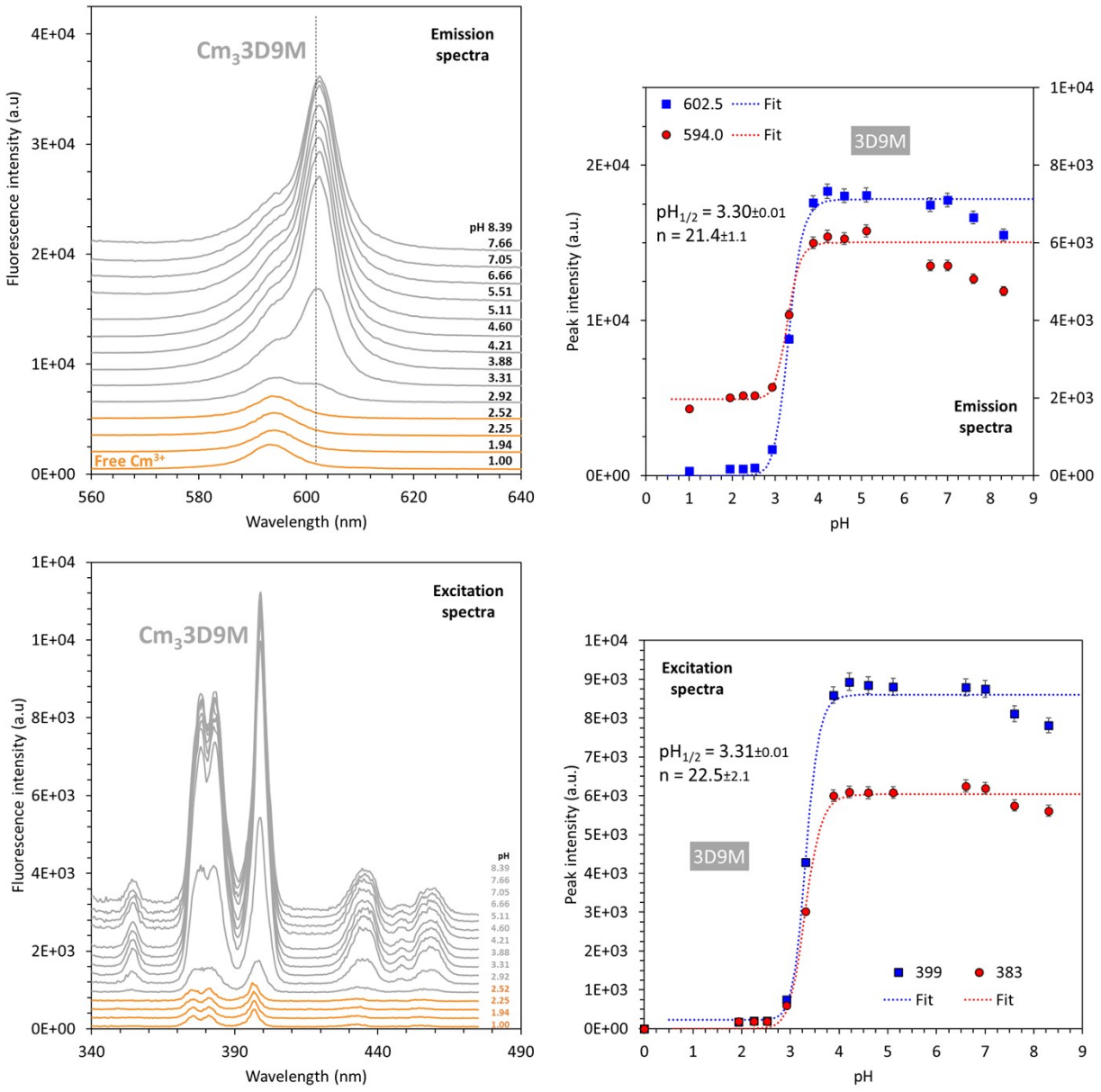

Figure S7. Fluorescence spectra of Cm(III) in the presence of the LanM variant $3D_9M$ and as a function of pH. Top panels = emission. Bottom panels = excitation. For clarity, spectra are stacked, with increasing pH from bottom to top. Right panels represent the measured fluorescence intensity as a function of pH and the corresponding fit results using the Hill equation. The spectral variations as a function of pH were fitted using the two main bands for the emission spectra (594 and 602.5 nm) and excitation spectra (383 and 399 nm). The values given are the average of the two displayed fits. The large *n* values confirm that the protein releases multiple metals, each from sites with multiple titrable ligands, under these conditions.

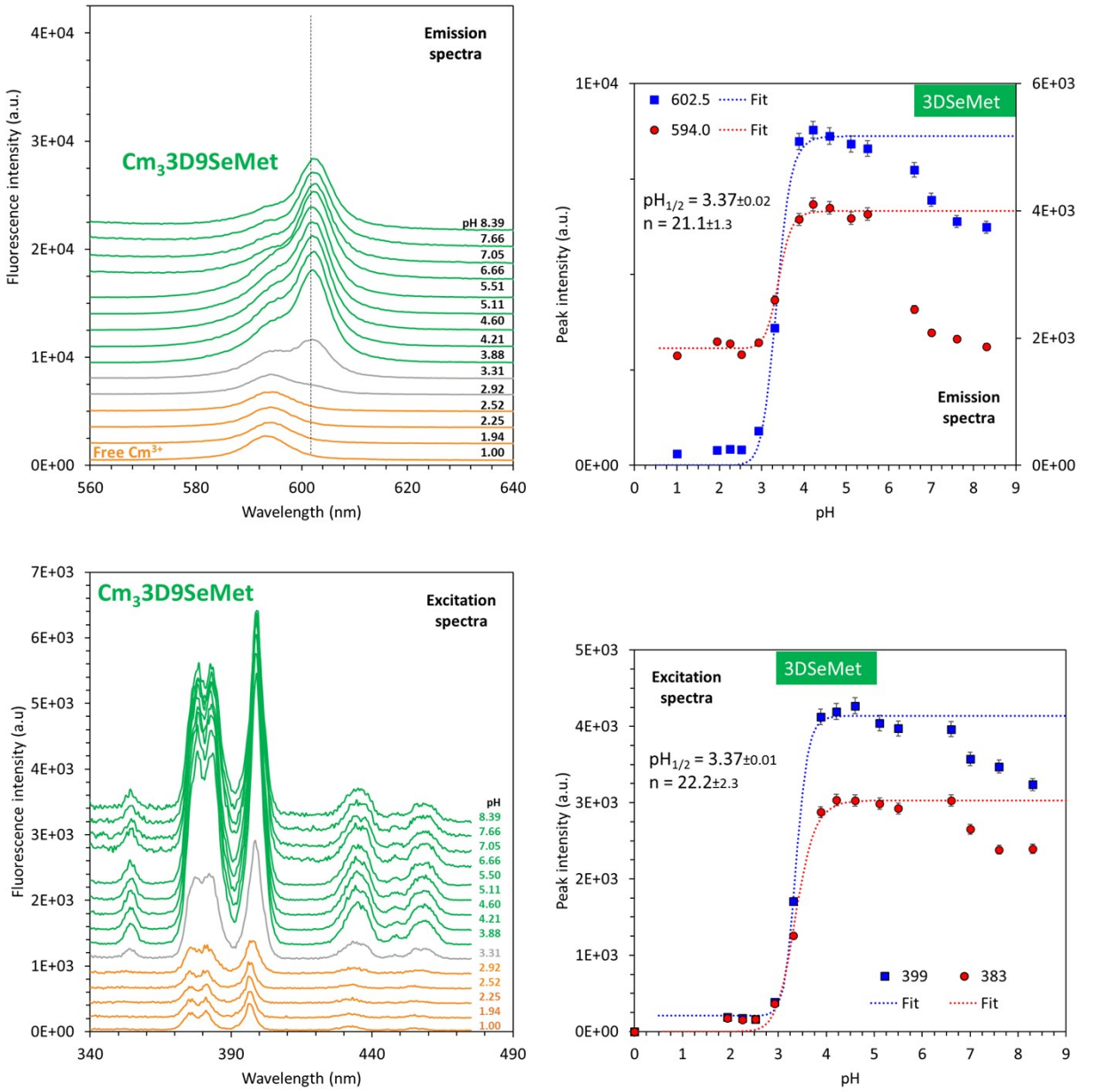

Figure S8. Fluorescence spectra of Cm(III) in the presence of the LanM variant 3D$_9$SeMet and as a function of pH. Top panels = emission. Bottom panels = excitation. For clarity, spectra are stacked, with increasing pH from bottom to top. Right panels represent the measured fluorescence intensity as a function of pH and the corresponding fit results using the Hill equation. The spectral variations as a function of pH were fitted using the two main bands for the emission spectra (594 and 602.5 nm) and excitation spectra (383 and 399 nm). The values given are the average of the two displayed fits. The large *n* values confirm that the protein releases multiple metals, each from sites with multiple titrable ligands, under these conditions.

Table S4. Curium fluorescence lifetimes in the presence of the LanM variants $3D_9N$ and $3D_9A$ and as a function of pH. These fluorescence measurements correspond to the experiments described in **Figure 4** and **Figures S4-S8**. λ_{em} = 399 nm. λ_{em} = 602 nm. The fluorescence decay curves were fitted with the minimal number of exponential functions (i.e., mono- or bi-exponential). As the pH decreases, the decay curve becomes bi-exponential with a short lifetime of ~85 µsec (unbound Cm^{3+}) and a long lifetime (Cm-LanM complex), and then becomes a mono-exponential function again at pH <2.5 and only the short lifetime is observed (unbound Cm^{3+}). Lifetime values are in microseconds.

	pH	Lifetime 1	Contribution lifetime 1	Lifetime 2	Contribution lifetime 2	Chi^2	**Average lifetime**
$3D_9N$	**1.00**	0.00	100%	/	0%	1.11	**0.00**
	1.94	68.94	100%	/	0%	0.91	**68.94**
	2.25	71.74	100%	/	0%	0.93	**71.74**
	2.52	65.22	53%	195.83	47%	0.90	**127.10**
	2.92	/	0%	193.28	100%	0.99	**193.28**
	3.31	/	0%	194.61	100%	0.99	**194.61**
	3.88	/	0%	193.49	100%	1.03	**193.49**
	4.21	/	0%	195.54	100%	0.85	**195.54**
	4.60	/	0%	191.25	100%	0.94	**191.25**
	5.11	/	0%	191.90	100%	1.02	**191.90**
	6.66	/	0%	193.51	100%	1.04	**193.51**
	7.05	/	0%	193.97	100%	1.04	**193.97**
	7.66	/	0%	192.67	100%	1.07	**192.67**
	8.30	/	0%	194.18	100%	1.02	**194.18**

	pH	Lifetime 1	Contribution lifetime 1	Lifetime 2	Contribution lifetime 2	Chi^2	**Average lifetime**
$3D_9A$	**1.00**	0.00	100%	/	0%	1.11	**0.00**
	1.94	68.94	100%	/	0%	0.91	**68.94**
	2.25	69.26	100%	/	0%	1.10	**69.26**
	2.52	70.61	100%	/	0%	0.90	**70.61**
	2.92	75.07	22%	211.40	78%	0.87	**181.61**
	3.31	/	0%	214.00	100%	0.88	**214.00**
	3.88	/	0%	217.83	100%	1.01	**217.83**
	4.21	/	0%	216.61	100%	0.99	**216.61**
	4.60	/	0%	215.15	100%	0.93	**215.15**
	5.11	/	0%	215.28	100%	1.09	**215.28**
	5.51	/	0%	214.68	100%	1.05	**214.68**
	6.66	/	0%	217.40	100%	0.97	**217.40**
	7.05	/	0%	216.39	100%	0.98	**216.39**
	7.66	/	0%	215.86	100%	0.94	**215.86**
	8.30	/	0%	213.98	100%	0.87	**213.98**

Table S5. Curium fluorescence lifetimes in the presence of the LanM variants $3D_9H$, $3D_9M$ and $3D_9SeMet$ and as a function of pH, similar to **Table S4**. Lifetime values are in microseconds. Table continues on the following page.

	pH	Lifetime 1	Contribution lifetime 1	Lifetime 2	Contribution lifetime 2	Chi^2	Average lifetime
$3D_9H$	**1.00**	0.00	100%	/	0%	1.11	**0.00**
	1.94	68.73	100%	/	0%	0.84	**68.73**
	2.25	68.59	100%	/	0%	0.88	**68.59**
	2.52	68.97	100%	/	0%	0.93	**68.97**
	2.92	71.43	93%	221.73	7%	0.97	**82.37**
	3.31	54.85	24%	230.97	76%	0.94	**189.38**
	3.88	/	0%	246.72	100%	0.97	**246.72**
	4.21	/	0%	249.75	100%	0.91	**249.75**
	4.60	/	0%	247.67	100%	0.93	**247.67**
	5.11	/	0%	242.92	100%	1.09	**242.92**
	6.66	/	0%	236.31	100%	1.07	**236.31**
	7.05	/	0%	234.62	100%	0.98	**234.62**
	7.66	/	0%	224.95	100%	1.08	**224.95**
	8.39	/	0%	223.58	100%	1.17	**223.58**

	pH	Lifetime 1	Contribution lifetime 1	Lifetime 2	Contribution lifetime 2	Chi^2	Average lifetime
$3D_9M$	**1.00**	0.00	100%	/	0%	1.11	**0.00**
	1.94	68.31	100%	/	0%	0.79	**68.31**
	2.25	69.03	100%	/	0%	0.84	**69.03**
	2.52	69.79	100%	/	0%	0.90	**69.79**
	2.92	67.82	51%	209.76	49%	0.94	**136.94**
	3.31	/	0%	215.32	100%	1.06	**215.32**
	3.88	/	0%	222.74	100%	0.98	**222.74**
	4.21	/	0%	221.59	100%	1.01	**221.59**
	4.60	/	0%	221.24	100%	0.84	**221.24**
	5.11	/	0%	218.46	100%	0.89	**218.46**
	6.60	/	0%	220.02	100%	0.94	**220.02**
	7.00	/	0%	220.61	100%	0.99	**220.61**
	7.60	/	0%	218.25	100%	1.05	**218.25**
	8.30	/	0%	216.57	100%	1.08	**216.57**

	pH	Lifetime 1	Contribution lifetime 1	Lifetime 2	Contribution lifetime 2	Chi^2	Average lifetime
$3D_9SeMet$	**1.00**	0.00	100%	/	0%	1.11	**0.00**
	1.94	68.94	100%	/	0%	0.91	**68.94**
	2.25	69.72	100%	/	0%	1.14	**69.72**
	2.52	69.67	100%	/	0%	0.92	**69.67**
	2.92	76.47	100%	/	0%	0.99	**76.47**
	3.31	62.82	21%	212.78	79%	1.11	**181.21**
	3.88	/	0%	219.21	100%	1.21	**219.21**

	4.21	/	0%	216.10	100%	1.01	**216.10**
	4.60	/	0%	214.62	100%	1.02	**214.62**
	5.11	/	0%	210.06	100%	0.98	**210.06**
	5.51	/	0%	208.64	100%	0.93	**208.64**
	6.66	/	0%	217.19	100%	1.11	**217.19**
	7.05	/	0%	216.30	100%	1.12	**216.30**
	7.66	/	0%	215.82	100%	0.93	**215.82**
	8.66	/	0%	213.62	100%	0.94	**213.62**

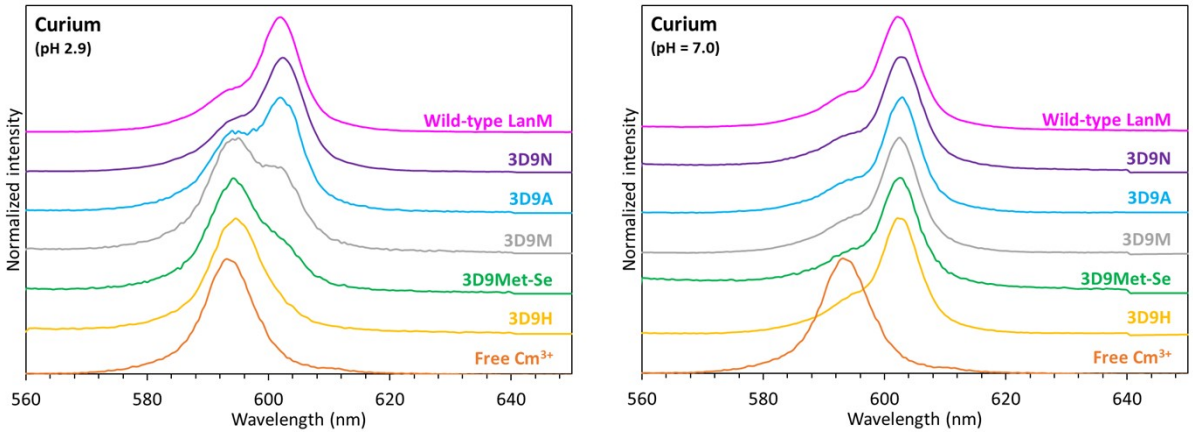

Figure S9. Comparison of the fluorescence spectra of curium(III) (1.0 µM) in the presence of wild-type LanM and its variants ($3D_9N$, $3D_9A$, $3D_9A$, $3D_9SeMet$, and $3D_9H$; 0.5 µM), at pH 2.9 (left) and at pH 7.0 (right). Spectra are normalized relative to the highest peak intensity. Without normalization, the free Cm(III) emission intensities are ~10 times lower than those of the Cm(III)-LanM complexes. See **Figure 4** and main text for more details.

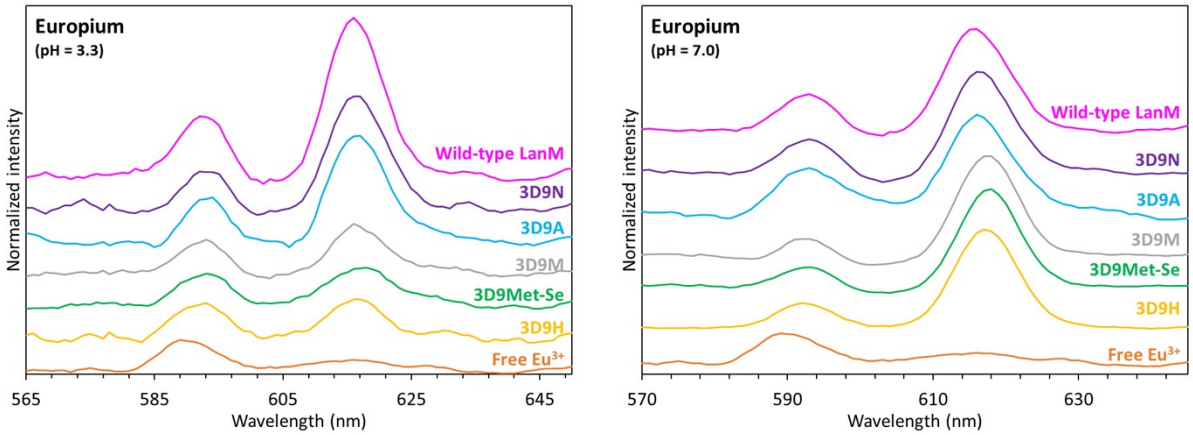

Figure S10. Comparison of the fluorescence spectra of europium(III) (1.0 µM) in the presence of wild-type LanM and its variants ($3D_9N$, $3D_9A$, $3D_9A$, $3D_9SeMet$, and $3D_9H$; 0.5 µM), at pH 3.3 (left) and at pH 7.0 (right). See **Figure 4** and main text for more details.

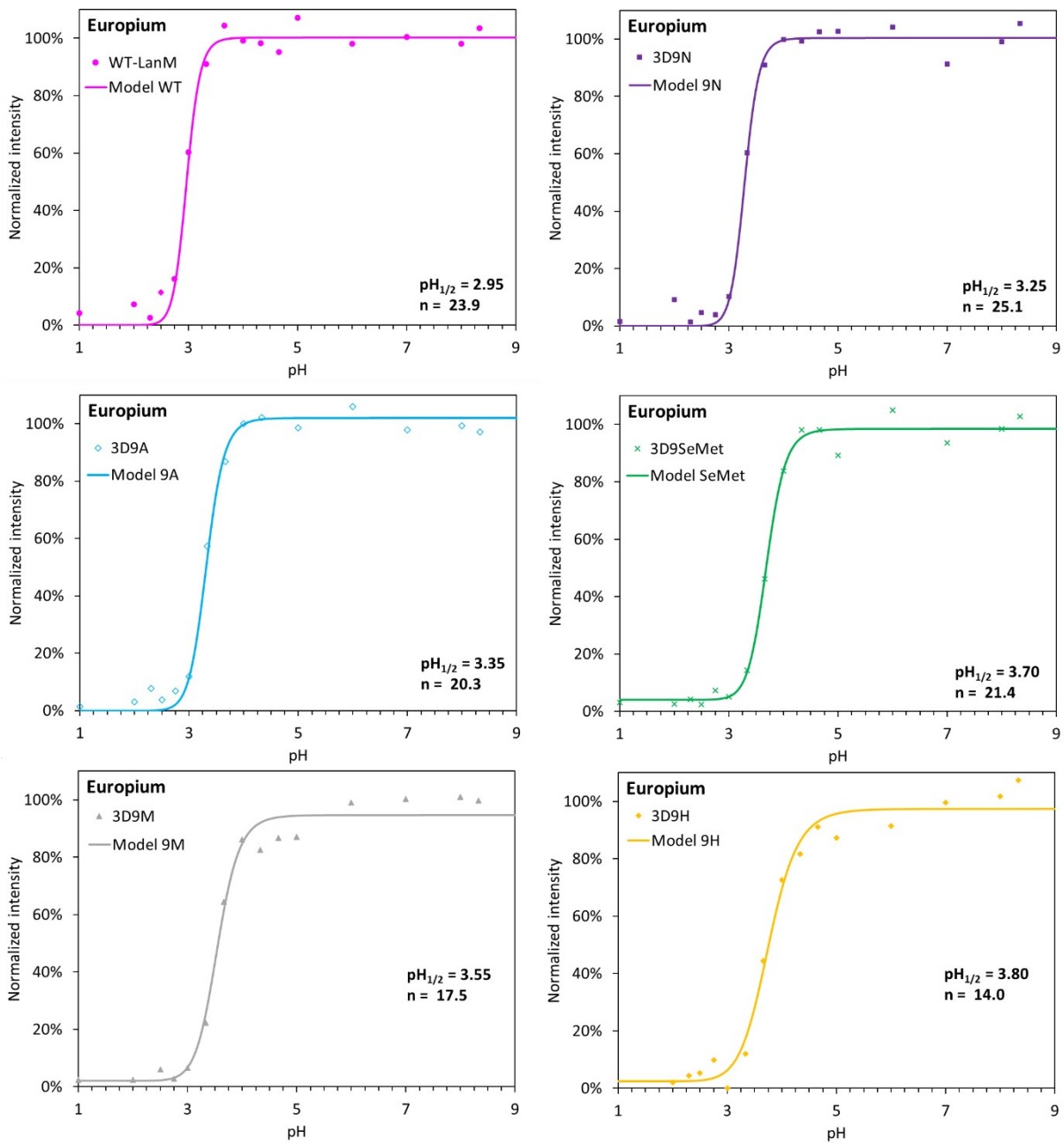

Figure S11. Comparison Fluorescence titration of Eu(III) in the presence of the WT LanM or its variants $3D_9N$, $3D_9A$, $3D_9M$, $3D_9H$, and $3D_9SeMet$, as a function of pH. The peak intensity (λ_{max} = 615 nm) is plotted as a function of pH. Each curve was fitted with Hill equation and the results fit parameter ($pH_{1/2}$ and n) are indicated on each graph. Symbols = experimental data. Solid lines = fitted curves.

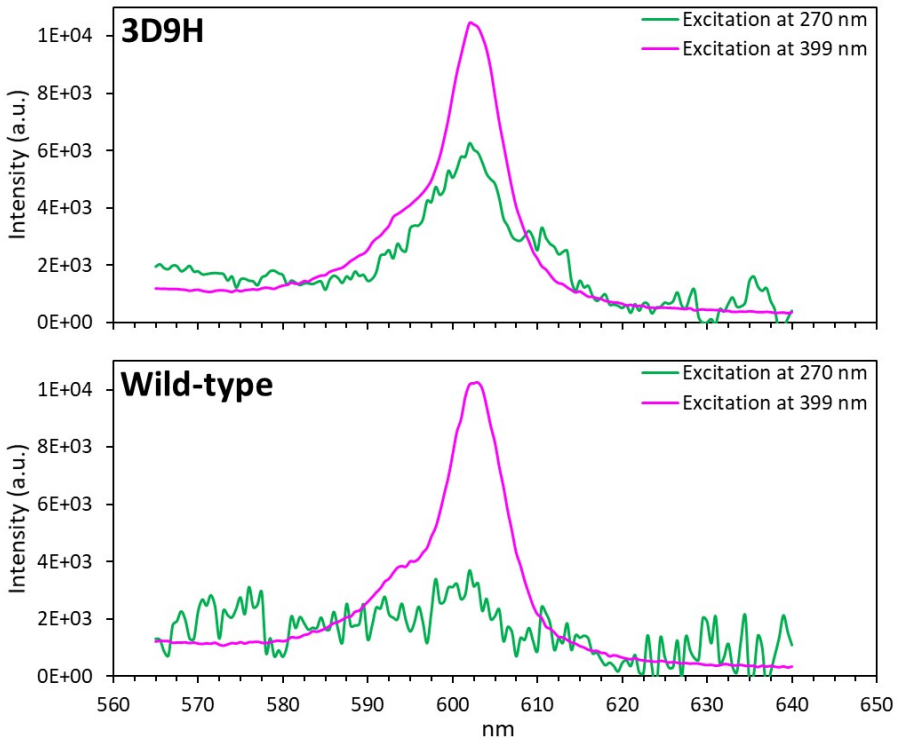

Figure S12. Comparison of the fluorescence emission of curium when bound to the $3D_9H$ variant and wild-type LanM. Pink curves: direct excitation of Cm(III) at 399 nm. Green curves: excitation of 270 nm. pH = 8.0. [Cm] = 1.0 µM, [LanM] = 0.5 µM. The lower signal-to-noise ratio for the green curves is due to the lower efficiency of fluorescence lamps in the low-wavelength region. Wild-type and $3D_9H$ samples were collected under identical conditions for a direct comparison.

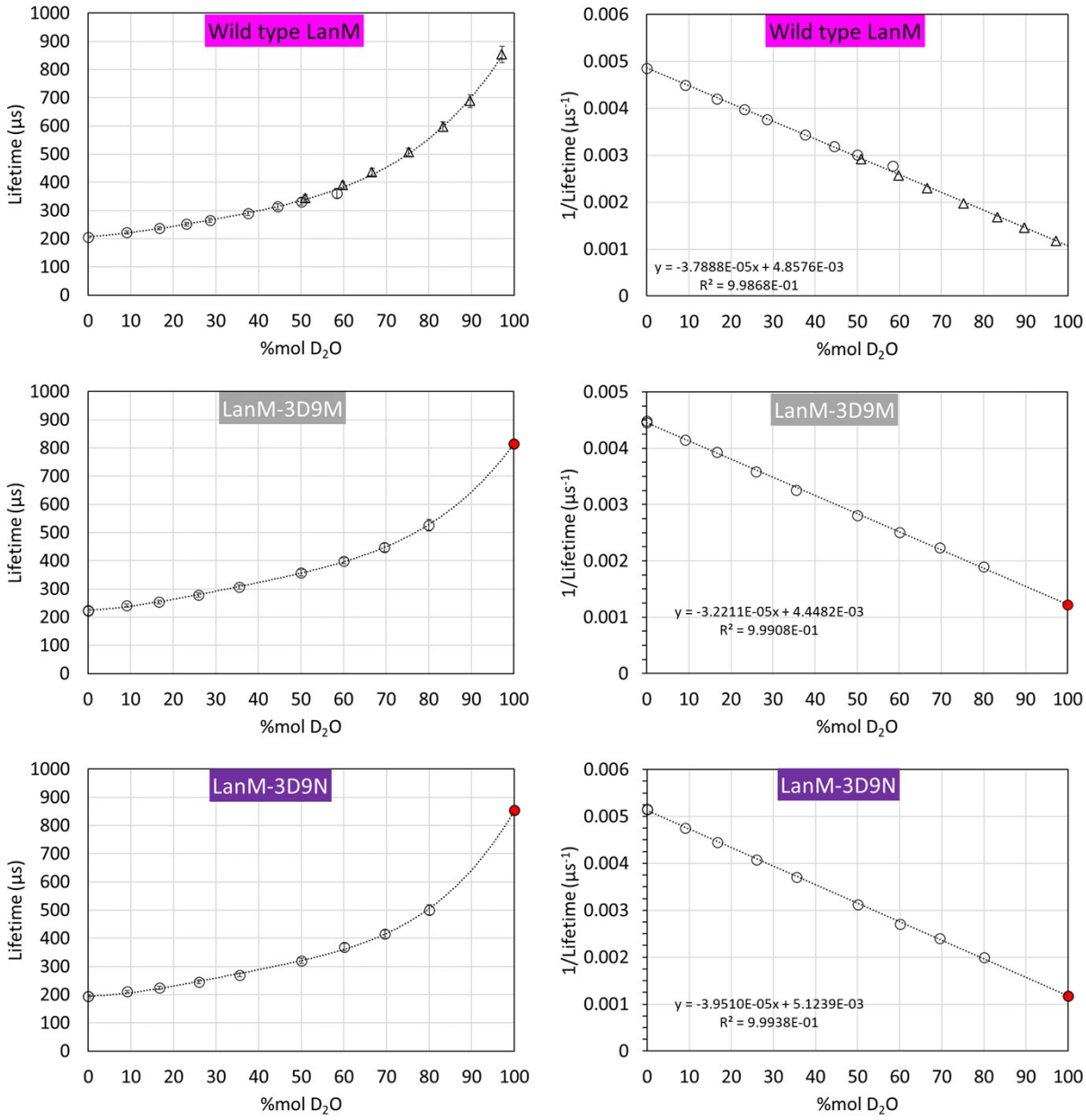

Figure S13. Fluorescence lifetime measurements for curium(III) when complexed to wild-type LanM, and its $3D_9M$ and $3D_9N$ variants, as a function of the content of D_2O (Initial pH = 7.0, buffer = 25 mM HEPES, 75 mM NaCl). Left panels: Lifetime value as a function of the D_2O content in solution. Right panels: linear correlation between 1/lifetime and the D_2O content in solution, and associated correlation coefficient. The points highlighted in red are extrapolated from the linear correlation.

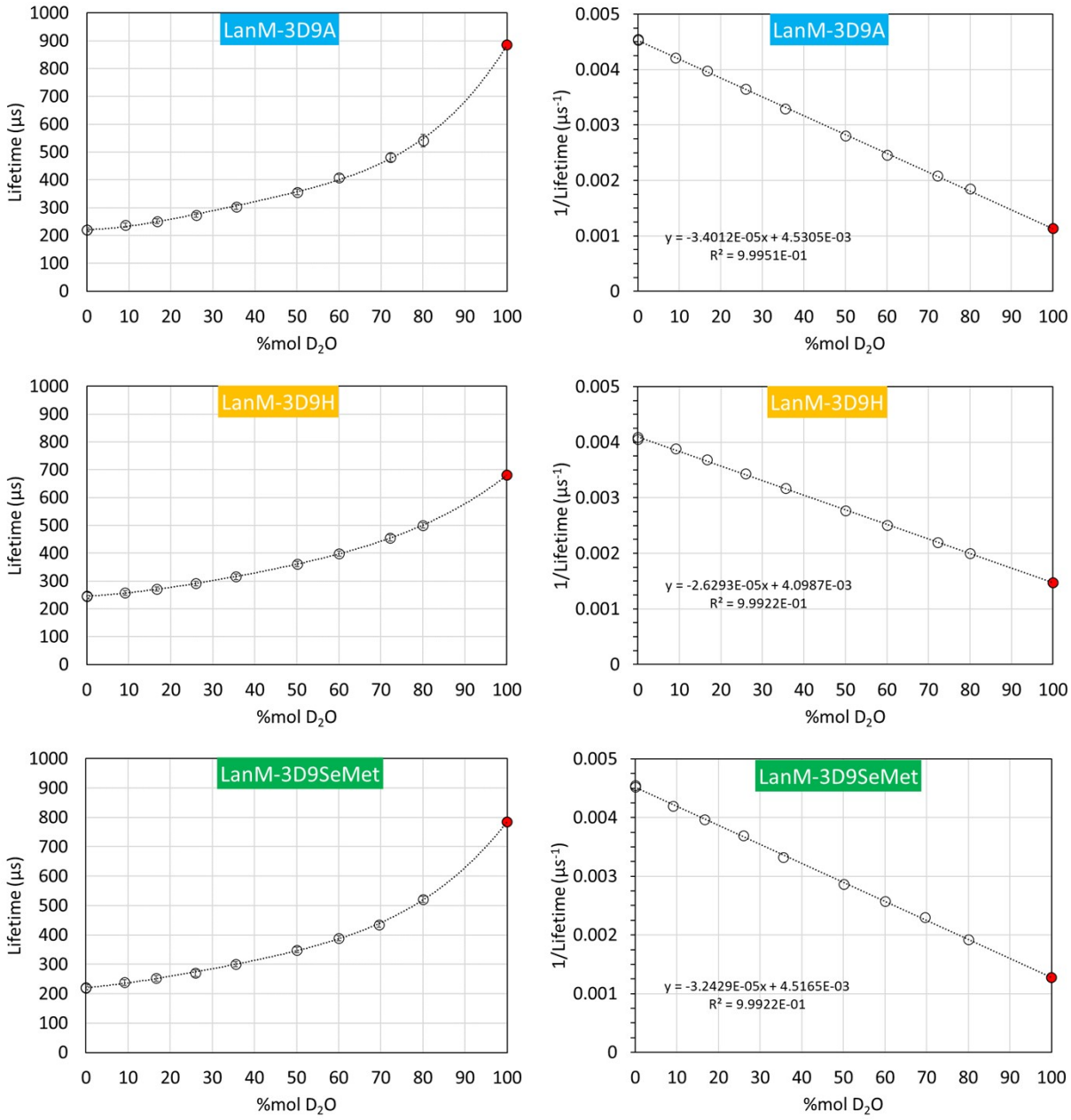

Figure S14. Fluorescence lifetime measurements for curium(III) when complexed to the $3D_9A$, $3D_9H$, and $3D_9SeMet$ variants of LanM, as a function of the content of D_2O (Initial pH = 7.0, buffer = 25 mM HEPES, 75 mM NaCl). Left panels: Lifetime value as a function of the D_2O content in solution. Right panels: linear correlation between 1/lifetime and the D_2O content in solution, and associated correlation coefficient. The points highlighted in red are extrapolated from the linear correlation.

Table S6. Curium fluorescence lifetimes in the presence of the LanM variants ($3D_9N$, $3D_9A$, $3D_9H$, $3D_9SeMet$, and $3D_9M$) measured in binary mixtures of H_2O-D_2O. The value for 100% D_2O is extrapolated from the other points, as shown in the right panels of **Figures S12 and S13**. Corresponding values for wild-type LanM have been reported elsewhere.[10]

	$3D_9N$		**$3D_9A$**		**$3D_9H$**		**$3D_9MetSe$**		**$3D_9M$**	
%mol D_2O	Lifetime (µs)	Chi^2	Lifetime (µs)	Chi^2	Lifetime (µs)	Chi^2	Lifetime (µs)	Chi^2	Lifetime (µs)	Chi^2
0.0	194.35	0.95	219.38	1.02	245.42	0.93	219.81	0.94	224.40	1.06
9.1	210.30	1.03	237.53	0.99	257.39	0.82	238.15	0.93	241.29	1.11
16.7	224.67	1.02	251.26	0.88	271.21	0.82	252.34	0.97	254.10	1.01
26.0	245.44	1.05	273.97	0.96	291.06	0.88	270.50	1.13	278.61	1.06
35.5	270.09	1.06	303.23	1.11	315.57	0.97	300.93	0.86	306.90	1.08
50.1	319.91	1.10	356.30	1.00	361.34	0.98	348.72	1.00	356.76	1.07
60.0	369.01	1.12	407.16	0.93	398.53	0.95	389.07	0.91	399.57	0.90
69.6	415.74	0.88	480.28	1.03	455.29	1.07	434.78	0.96	447.62	0.94
80.0	500.23	1.02	541.58	1.01	500.44	0.96	521.32	1.04	526.34	1.05
100	852.59	/	885.50	/	680.55	/	785.18		814.93	/

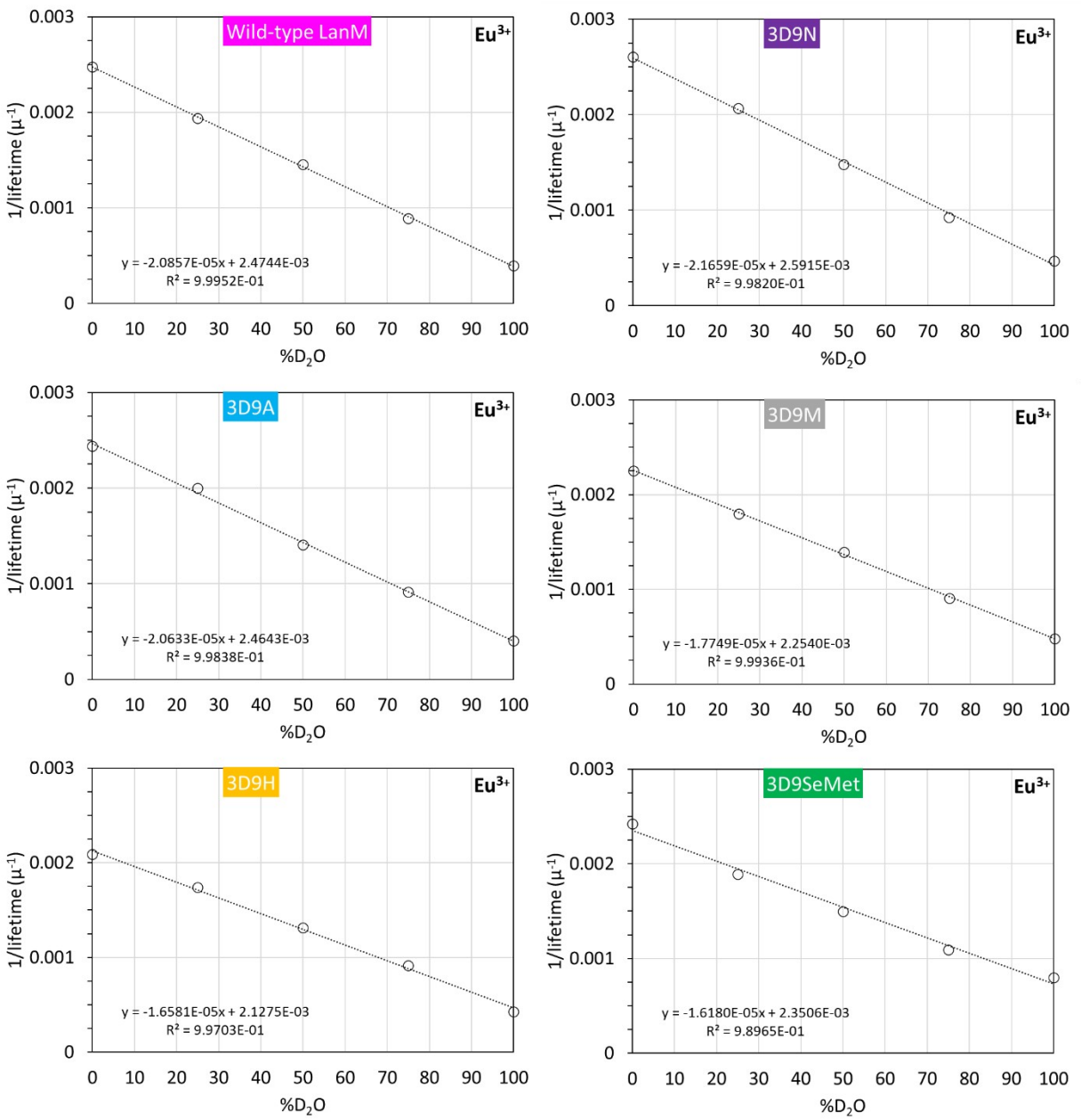

Figure S15. Fluorescence lifetime measurements for europium(III) when complexed to wild-type LanM, or its variants $3D_9N$, $3D_9A$, $3D_9M$, $3D_9H$, and $3D_9SeMet$, as a function of the content of D_2O.

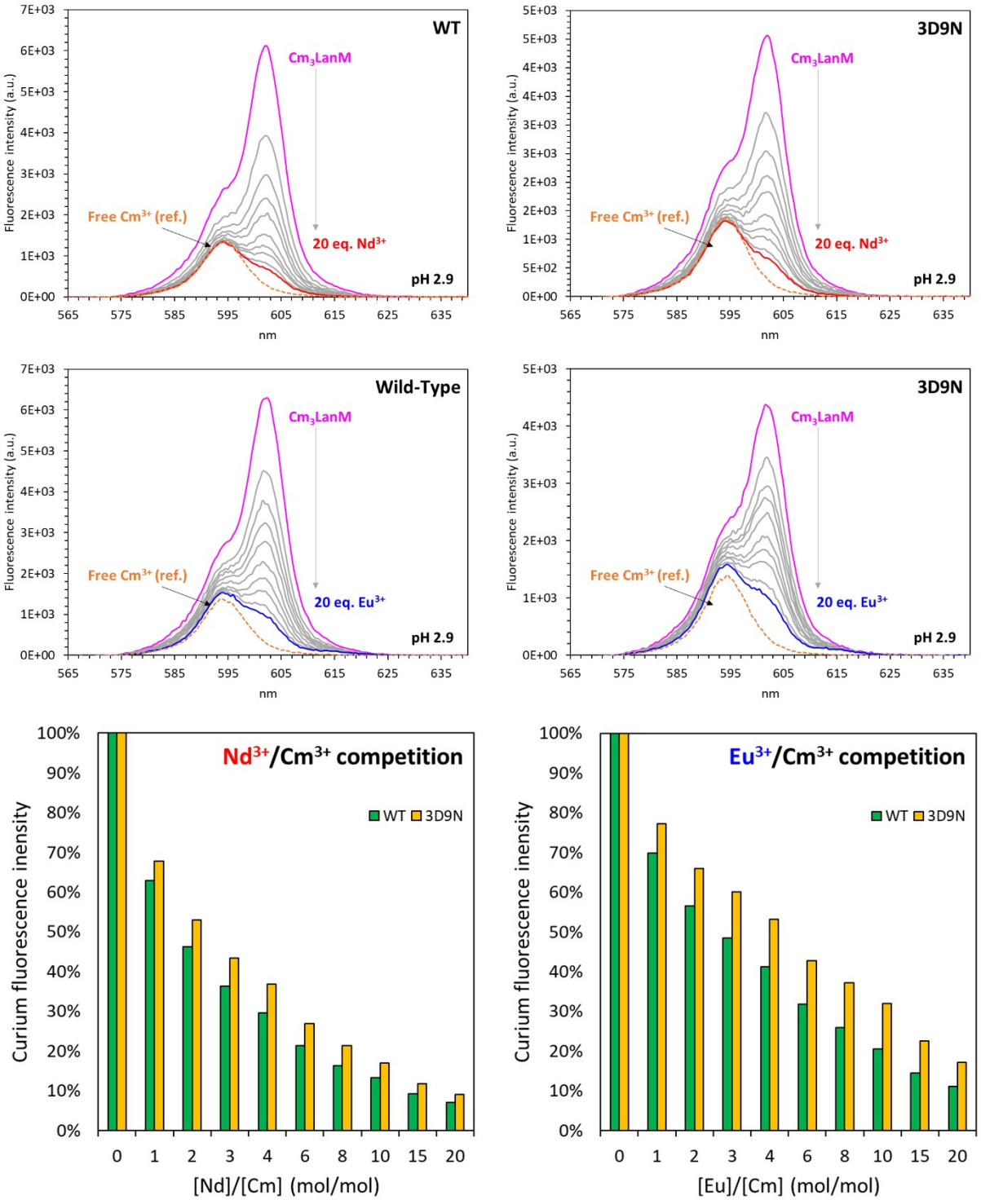

Figure S16. Observed selectivity of wild-type LanM and its variant 3D$_9$N for the trivalent actinide, Cm^{3+}, over the trivalent lanthanides (Nd^{3+} and Eu^{3+}). Top panels: Nd/Cm competition followed by fluorescence spectroscopy. Middle panels: Eu/Cm competition. Bottom panels: Fluorescence intensity of the Cm-LanM complexes' peak (centered at 602.5nm) as a function of the ratio Nd/Cm (left) or Eu/Cm (right). pH = 2.9. T = 22 °C. Buffer: 25 mM glycine, 75 mM NaCl.

Supplementary References

1 J. A. Mattocks, J. L. Tirsch and J. A. Cotruvo, in *Methods in Enzymology*, ed. J. A. Cotruvo, Academic Press, 2021, vol. 651, pp. 23–61.

2 E. R. Featherston, H. R. Rose, M. J. McBride, E. M. Taylor, A. K. Boal and J. A. Cotruvo Jr., *ChemBioChem*, 2019, **20**, 2360–2372.

3 R. M. Smith and A. E. Martell, in *Critical Stability Constants: Second Supplement*, eds. R. M. Smith and A. E. Martell, Springer US, Boston, MA, 1989, pp. 1–66.

4 S. G. Johnson, *NIST46 - NIST Critically Selected Stability Constants of Metal Complexes:*, National Institute of Standards and Technology, Gaithersburg, MD. USA, 2013.

5 W. H. Runde and W. W. Schulz, in *The Chemistry of the Actinide and Transactinide Elements*, eds. L. R. Morss, N. M. Edelstein and J. Fuger, Springer Netherlands, Dordrecht, 2006, pp. 1265–1395.

6 J. A. Jr. Cotruvo, E. R. Featherston, J. A. Mattocks, J. V. Ho and T. N. Laremore, *J. Am. Chem. Soc.*, 2018, **140**, 15056–15061.

7 L. Alderighi, P. Gans, A. Ienco, D. Peters, A. Sabatini and A. Vacca, *Coordination Chemistry Reviews*, 1999, **184**, 311–318.

8 G. J.-P. Deblonde, J. A. Mattocks, D. M. Park, D. W. Reed, J. A. Cotruvo and Y. Jiao, *Inorg. Chem.*, 2020, **59**, 11855–11867.

9 G. J.-P. Deblonde, in *Methods in Enzymology*, Academic Press, 2021.

10 G. J.-P. Deblonde, J. A. Mattocks, H. Wang, E. M. Gale, A. B. Kersting, M. Zavarin and J. A. Cotruvo, *J. Am. Chem. Soc.*, 2021, **143**, 15769–15783.

11 D. Chaudhuri, W. DeW. Horrocks, J. C. Amburgey and D. J. Weber, *Biochemistry*, 1997, **36**, 9674–9680.

12 E. R. Featherston, E. J. Issertell and J. A. Cotruvo, *J. Am. Chem. Soc.*, 2021, **143**, 14287–14299.